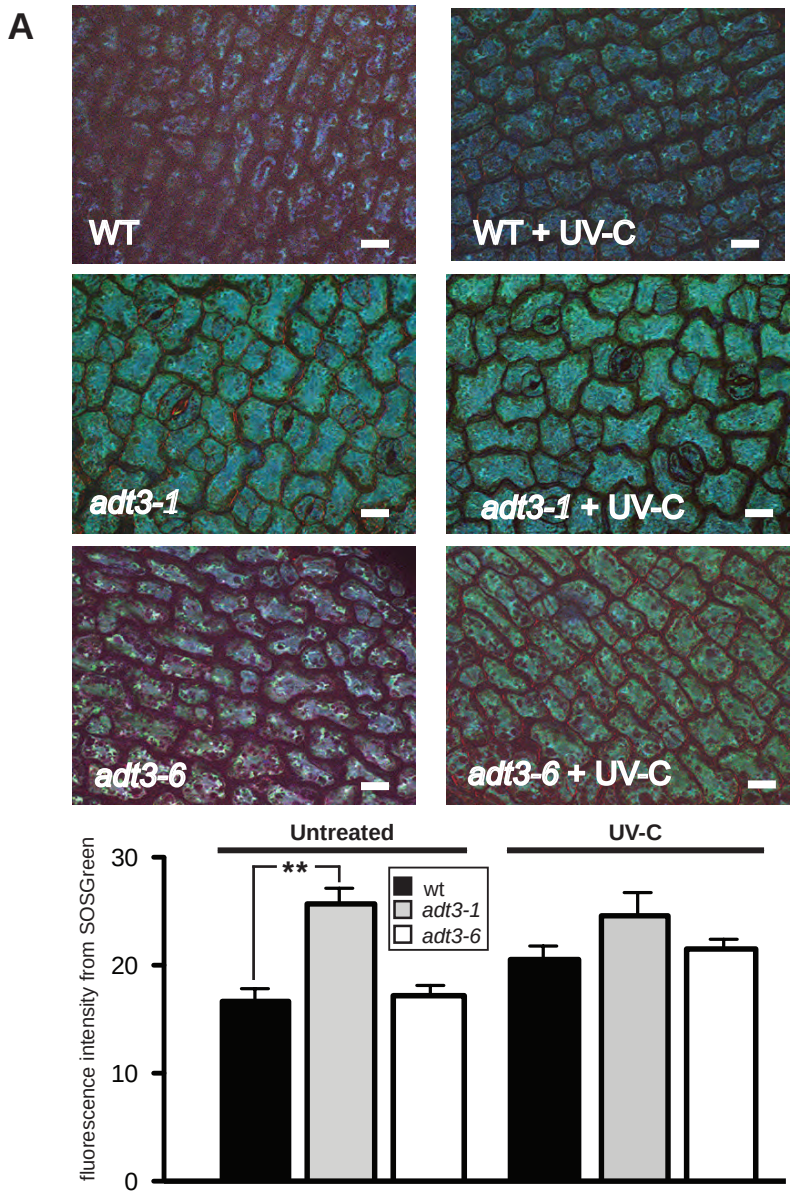

Figure S4. Singlet oxygen species (SOS) detection in *adt3* mutant seedlings incubated with Singlet Oxygen Sensor Green™ (SOSG).

A. Seedlings were grown and treated as described for Fig. 2. Merged (DAPI, FITC and Texas Red) images of the cotyledon epidermis of live 6-d-old dark-grown seedlings treated SOSG with are shown. WT and *adt3-1* unirradiated and were either mock irradiated (control)(left panels), or irradiated with 254nm (UV-C)(right panels) then immediately incubated in SOSG, washed, then imaged on the deconvoluting microscope in the epidermal plane. Scale bars = 10µm. FITC fluorescence (false-colored green) from the activated SOSG was quantitated (relative fluorescence, artificial units) in PC using ImageJ (bar graph, bottom panel). Each bar represents min 6 quantitated cells of 4 replicates, where each replicate =20 representative seedlings. Error bars are SEM. ** = $p<0.01$.

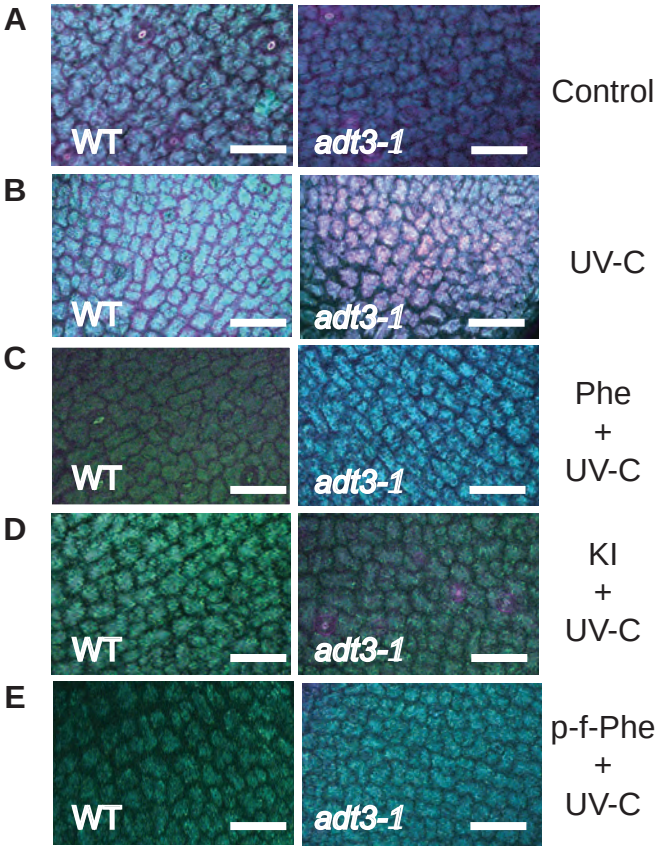

Figure S5. ROS levels detected by CellRox™ from unirradiated and UV-C irradiated WT and *adt3-1* seedling cotyledons before and after pre-treatment with Phe, the ROS scavenger KI and a Phe analog.

Seedlings of WT and *adt3-1* were grown and treated as described for Fig. 2, then imaged at 20X. Optical sections of the epidermis of 6 d, dark-grown WT (left) and *adt3-1* (right) seedlings stained with CellRox™ Deep Red are shown. Merged (DAPI, FITC and Cy5) images of **A**. No irradiation Control. **B**. UV-C (254nm) irradiated seedlings and seedlings pre-treated with **C**. Phe **D**. KI and **E**. p-f-Phe before UV-C irradiation. On day 6, seedlings growing on top agarose were lifted intact and moved to sterile filter paper containing 0.5X MS (control) (A and B) or 500µM exogenous Phe (C), KI (D) or the Phe analog p-f-Phe for 3h, irradiated as described for Fig. 2, then treated with CellRox™ and imaged in the same manner. A decrease of CellRox™ signal (false colored pink) in irradiated WT or *adt3-1* seedlings after pre-treatmentwith Phe, KI or the Phe analog p-f-Phe indicates that ROS scavenging has occurred. n=3 experiments of 30 seedlings viewed per replicate. Scale bar = 50 µm.

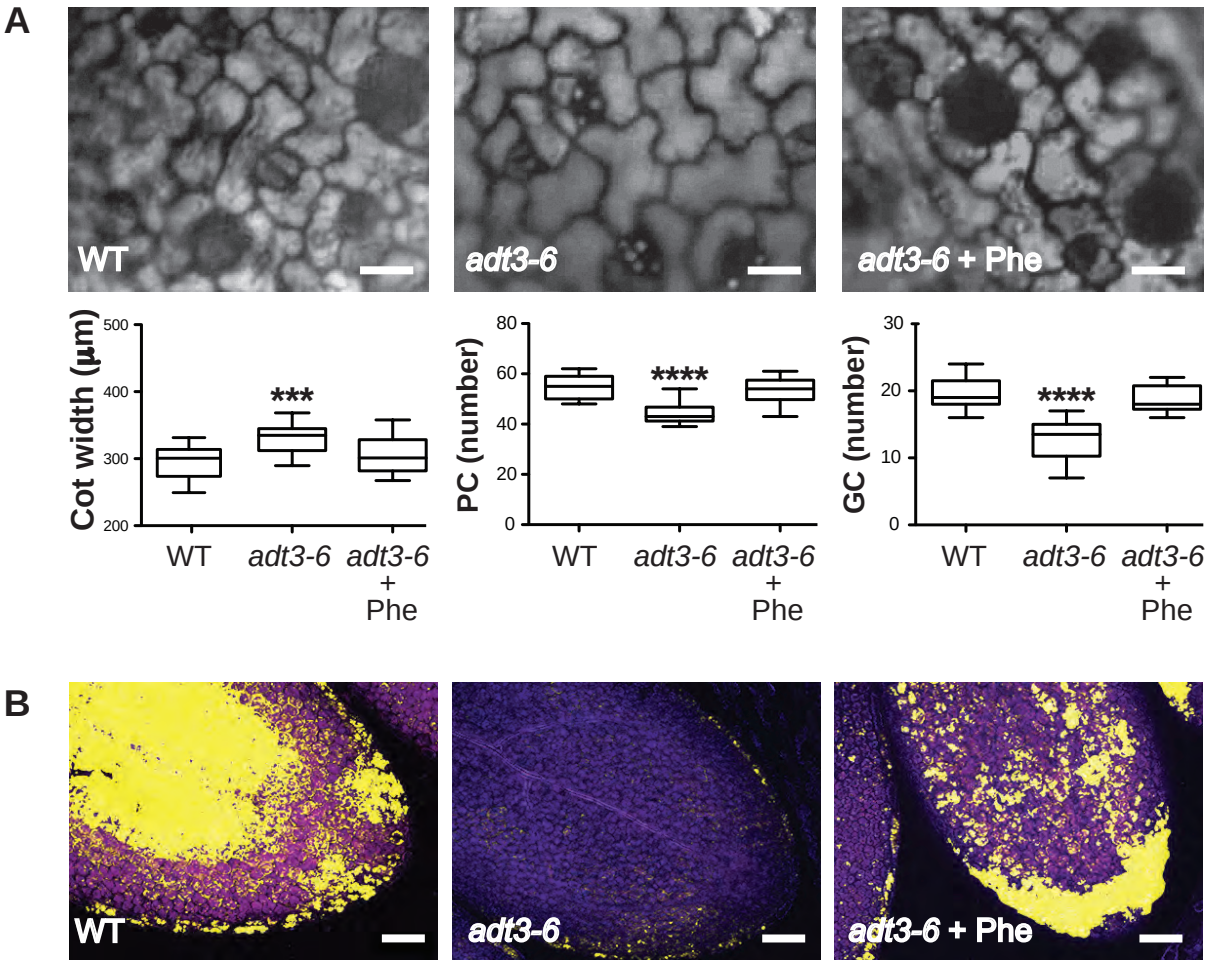

Figure S6. Epidermal defects in *adt3-6* seedlings are rescued by Phe.

Seedlings were grown and treated the same way as described for Fig. 3. **A**. Epidermis of WT (top left panel) and *adt3-6* (top middle and right panels) live cotyledons were viewed on a deconvoluting microscope (DAPI contrast). GC lineage (meristemoid and GC) cells are dark gray, and PCs appear light gray. Defects are prevented by inclusion of Phe in medium (*adt3-6* + Phe, top right panel). Scale bar = 10µm. Measurement of cotyledon width, PC number and GC number in WT and *adt3-6* without, and with added Phe are shown in the bottom panels. Cartoon indicates structured measured. *** = p<.001, **** = p<.0001. n=4 replicates (15-30 seedlings). **B**. Cotyledons of 6-d-old dark grown WT (left), *adt3-6* (middle) and *adt3-6* + Phe (right) seedling after staining with Nile Red (1µ m thick optical slice). Merges of DAPI (blue), FITC (gold) and CY5 (pink) are shown. n=3 (30 seedlings). Scale bar = 50µm.

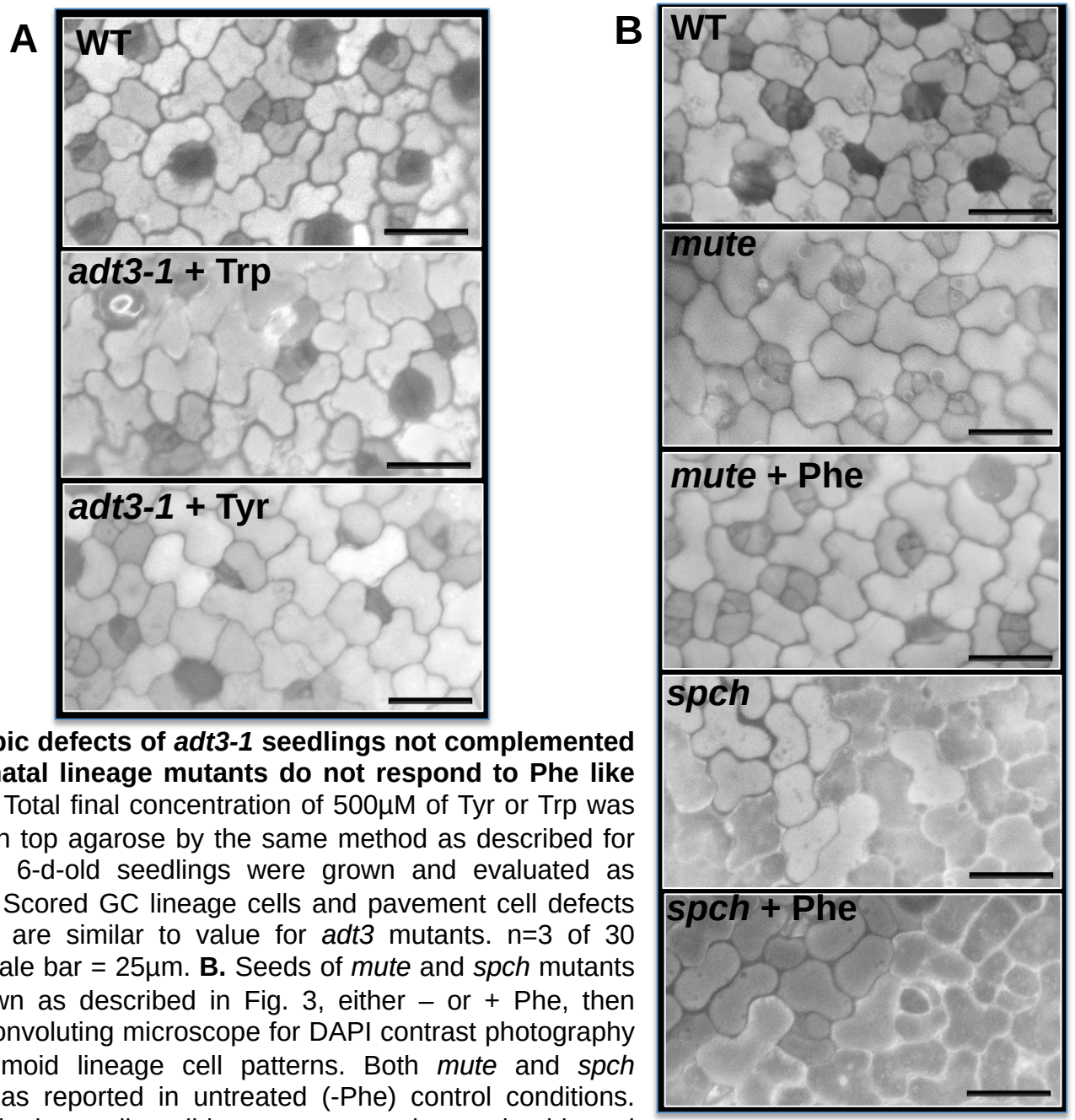

Figure S7. Phenotypic defects of *adt3-1* seedlings not complemented by Tyr or Trp; stomatal lineage mutants do not respond to Phe like *adt3-1* mutants. **A.** Total final concentration of 500µM of Tyr or Trp was incubated, included in top agarose by the same method as described for Phe (Fig. 3), where 6-d-old seedlings were grown and evaluated as described for Fig. 3. Scored GC lineage cells and pavement cell defects and cotyledon width are similar to value for *adt3* mutants. n=3 of 30 seedlings viewed; Scale bar = 25µm. **B.** Seeds of *mute* and *spch* mutants were sown and grown as described in Fig. 3, either – or + Phe, then viewed live on a deconvoluting microscope for DAPI contrast photography to view the meristemoid lineage cell patterns. Both *mute* and *spch* seedlings appeared as reported in untreated (-Phe) control conditions. The inclusion of Phe in the medium did not cause any observed epidermal changes. n=3 of 30; Scale bar = 25µm.

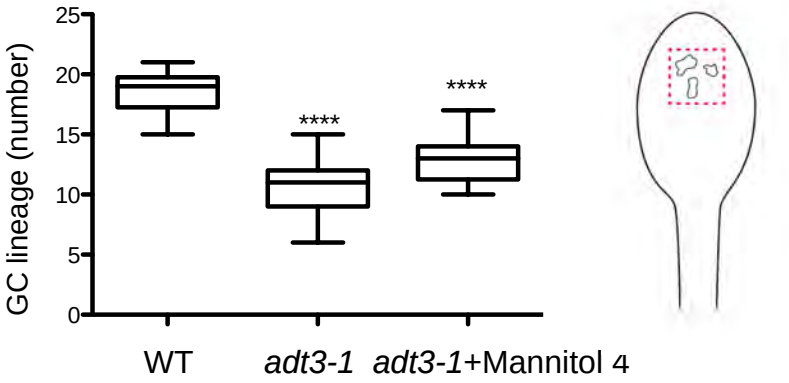

Figure S8. Experiments indicate mannitol does not rescue GC lineage progression.
Seedlings were grown as described in Fig. 6, At d 4 seedlings were transferred to filters containing 1% mannitol (controls were seedlings of WT and *adt3-1* which were transferred to 0.5XMS at d 4, then scored 48 h later, same as seedlings with mannitol treatment). 48h later (on d 6) seedlings were assessed for epidermal development and compared to WT and *adt3-1* untreated with sucrose. GC number were quantified n=3 sets of 30. **** <.0001.

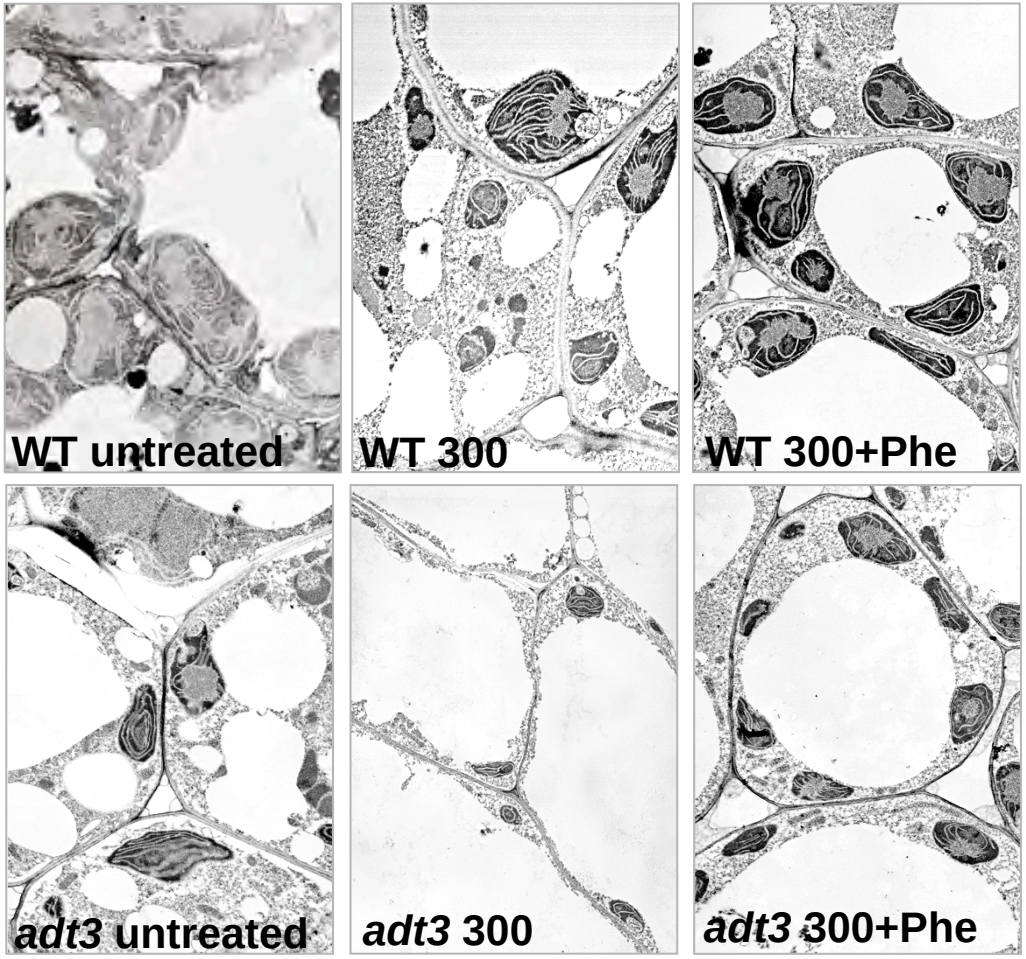

Figure S9. Developing chloroplast ultrastructural phenotype rescue in *adt3* mesophyll cells by inclusion of Phe in planting medium.
TEM micrographs of sections perpendicular to the adaxial surface of the cotyledons of 7-day old, dark-grown WT and *adt3-1* seedlings were prepared for TEM as described in Warpeha et al. 2008. (n=5 seedlings, ~100 cells observed). Scale bar = 2µm. On day 6 seedlings were treated with a brief pulse of 300nm UV (Warpeha et al., 2008), then 24 h later, seedlings were harvested for TEM.

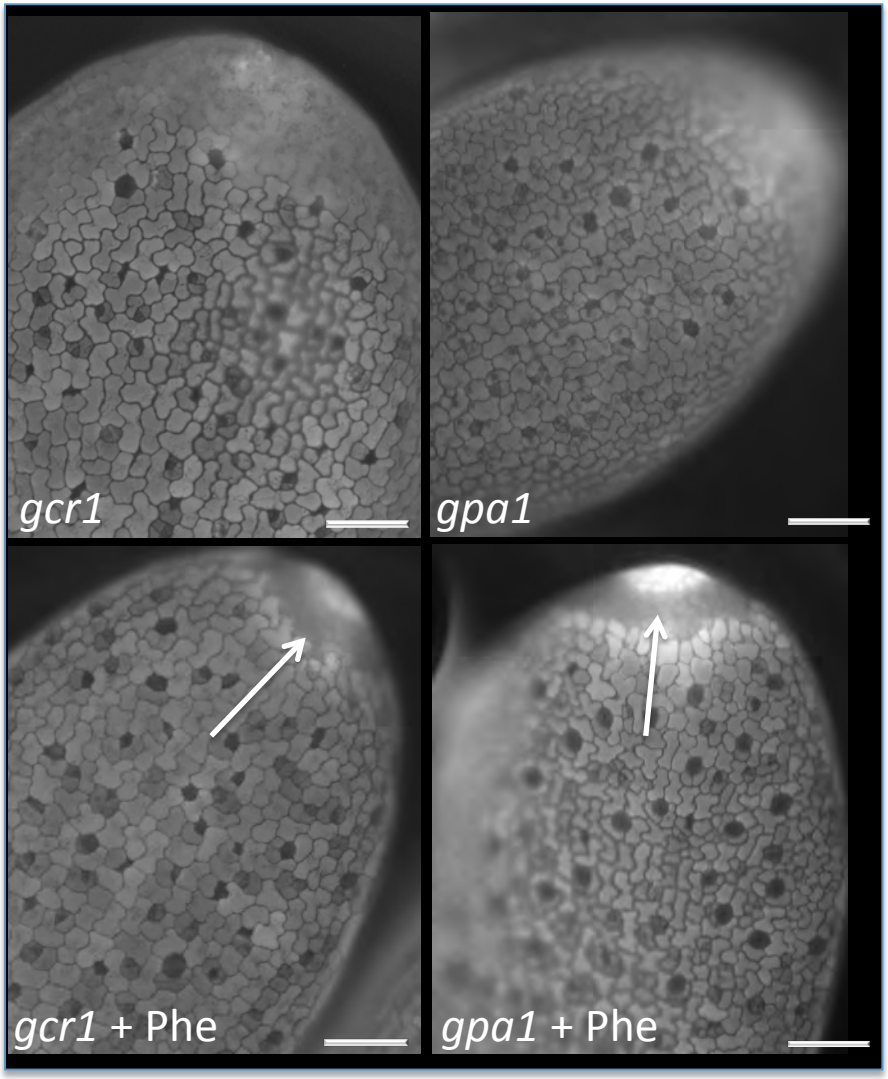

Figure S10. *gpa1* and *gcr1* mutants have cotyledon phenotypes that can be rescued by Phe. Seeds of *gcr1* and *gpa1* mutants were sown and grown as described in Fig. 3, then viewed live on a deconvoluting microscope for DAPI contrast photography to view the epidermis. When Phe was included in the top agarose from sowing (as is described for Fig. 3), the phenylpropanoid focus observed at the tip of the cotyledon was restored indicated by arrows (Warpeha et al., 2006; 2008), GC were more numerous and developed, and cotyledon width and cells were similar to WT (n=20; scale bar = 50µm).